

Strong-coupling superconductivity induced by calcium intercalation in bilayer transition-metal dichalcogenides

R. Szcześniak, A.P. Durajski,* and M.W. Jarosik
*Institute of Physics, Częstochowa University of Technology,
Ave. Armii Krajowej 19, 42-200 Częstochowa, Poland*

We theoretically investigate the possibility of achieving a superconducting state in transition-metal dichalcogenide bilayers through intercalation, a process previously and widely used to achieve metallization and superconducting states in novel superconductors. For the Ca-intercalated bilayers MoS₂ and WS₂, we find that the superconducting state is characterized by an electron-phonon coupling constant larger than 1.0 and a superconducting critical temperature of 13.3 and 9.3 K, respectively. These results are superior to other predicted or experimentally observed two-dimensional conventional superconductors and suggest that the investigated materials may be good candidates for nanoscale superconductors. More interestingly, we proved that the obtained thermodynamic properties go beyond the predictions of the mean-field Bardeen–Cooper–Schrieffer approximation and that the calculations conducted within the framework of the strong-coupling Eliashberg theory should be treated as those that yield quantitative results.

Keywords: 2D superconductivity, Effect of intercalation, Transition-metal dichalcogenides, Thermodynamic properties

PACS numbers: 74.20.Fg, 74.25.Bt, 74.62.Fj

I. INTRODUCTION

Superconductivity in two-dimensional (2D) materials has attracted considerable interest since it was noted that 2D monolayers may exhibit different properties than their corresponding bulk materials [1–3]. 2D superconductivity has been investigated for the past 80 years, and the research has provided insight into a variety of quantum phenomena such as localization of electrons and/or Cooper pairs [4], oscillations of order parameter and critical temperature caused by quantum size effects [5–7], transition from a superconducting to an insulating phase with increasing disorder or magnetic field [8] and Berezinskii–Kosterlitz–Thouless transition [9–11]. Recent advances in these materials have led to a variety of promising technologies for nanoelectronics, photonics, sensing, energy storage, and optoelectronics [12].

Over the past several years, special attention has been paid on transition-metal dichalcogenides (MX_2 , where $M = \text{Mo}$ or W , and $X = \text{S}$, Se , or Te) because of their fascinating physical properties and their potential for various applications. Particularly, molybdenum disulfide (MoS₂) has attracted significant interest [2, 13–18]. Bulk MoS₂ is a semiconductor with an indirect band gap of about 1.29 eV [19], while its monolayer form has a direct band gap of 1.90 eV [20]. This means that MoS₂ is a prime candidate for use in optoelectronic devices, transistors, and photodetectors [13, 21]. Similar to graphene [22–24], semiconducting layered transition-metal dichalcogenides can be metallized or even become superconductors upon alkali metal-atom intercalation or strain [25–27]. Theoretical research

has shown that Li- and Na-intercalated bilayer MoS₂ are promising conventional superconductors having superconducting transition temperatures of approximately 10.2 K and 2.8 K, respectively [27, 28]. More interestingly, T_C and electronic properties can be significantly enhanced by tensile strain [29]. In the case of (MoS₂)₂Na at 7%, biaxial tensile strain T_C increases to 10 K [27]. Experimentally, superconductivity in the MoS₂ transistor that adopts an electric double layer as a gate dielectric was successfully induced with a maximum T_C of approximately 10.8 K [30]. In addition, after external pressure was applied, iso-structural semiconducting to metallic transition in multilayered MoS₂ was observed at ~ 19 GPa [31], and the emergence of a superconducting state having the highest critical temperature among transition metal dichalcogenides (T_C of approximately 11.5 K above 120 GPa) was reported [32]. Unfortunately, from the technological point of view, such high pressure excludes MoS₂ from potential practical applications. Because of this, finding intercalants that, after being introduced into layered structures, allow for induction of a superconducting state with as high a critical temperature at normal pressure as possible [33–38] seems natural.

In the present study, we combine first-principles density functional theory and strong-coupling Eliashberg formalism for a comparative study of superconductivity in Ca-intercalated transition-metal dichalcogenide bilayers MoS₂ and WS₂. The choice of Ca as an intercalant was inspired by recent studies of experimentally observed superconductivity in Ca-intercalated bilayer graphene and Ca-doped graphene laminates with T_C of approximately 4 K and 6.4 K, respectively [39, 40]. Our results show that (MoS₂)₂Ca and (WS₂)₂Ca systems are phonon-mediated strong-coupling superconductors having critical temperatures of 13.3 and 9.3 K, respectively.

* adurajski@wip.pcz.pl

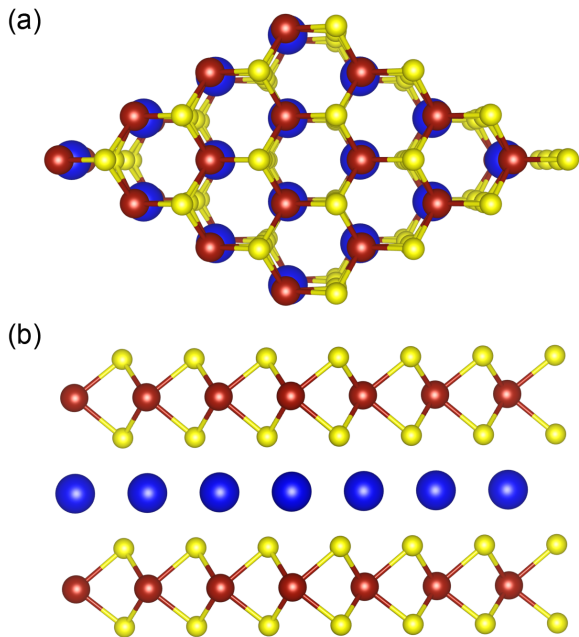


FIG. 1. Top (a) and front (b) view of the $(MS_2)_2Ca$ superconductor. The red, yellow, and blue spheres denote Mo (or W), S, and Ca atoms, respectively. In order to avoid any interaction between intercalated bilayers, we used the periodic boundary condition with a vacuum space of 20 Å along the non-periodic z direction.

II. COMPUTATIONAL DETAILS

First-principles studies are performed within the framework of the density functional theory (DFT) as implemented in the Quantum-ESPRESSO package [41–43]. The generalized gradient approximation (GGA) with the Perdew–Wang (PW91) exchange correlation function was used in our study. The plane-wave energy cutoff for the wavefunctions was set to 80 Ry. For the electronic structure investigations, the Brillouin zone was sampled using a set of $24 \times 24 \times 1$ Monkhorst–Pack k -mesh. A k -points grid of $60 \times 60 \times 1$ and a q -points grid of $6 \times 6 \times 1$ were used to calculate the electron-phonon coupling matrix and phonon spectrum. The single-layer of transition-metal dichalcogenide consists of one monoatomic hexagonal Mo or W plane placed between two monoatomic hexagonal S planes that are bonded together through weak van der Waals interactions [44]. Following intercalation, two transition-metal dichalcogenide layers were separated by foreign-atoms layer. By performing structural relaxation, we confirmed that for the most stable structure of bilayers MoS_2 and WS_2 intercalated by Ca atoms, the top and bottom monolayers are mirror images of each other and the intercalated Ca atoms have the same configuration as that of the Mo or W atoms (see Fig. 1). The previously conducted first-principles calculations show that, from among three possible stacking orders, this structure is dynamically stable for Li-intercalated bilayer MoS_2 [28]. The total energy of $(MoS_2)_2Ca$ as a function of the volumes for three

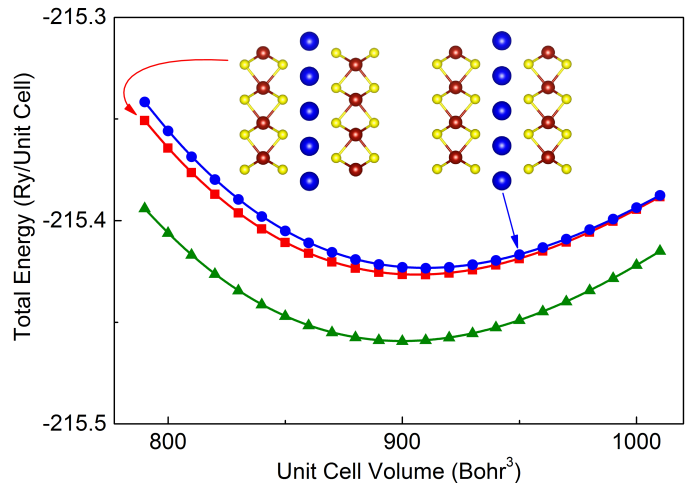


FIG. 2. The calculated total energy vs. volumes for three possible stacking orders of Ca-intercalated bilayer MoS_2 (the green line corresponds to the structure presented in Fig. 1).

different structural types are given in Fig. 2. We can see that the structure from Fig. 1 has lower total energy at an equilibrium volume. The presence of imaginary phonon frequencies indicates structural instability. The calculated phonon dispersion and phonon density of states (PhDOS) of Ca-intercalated bilayer molybdenum and tungsten disulfides are shown in Fig. 3. We can see that no negative frequencies exist, thus confirming the dynamical stability of the structure from Fig. 1. Therefore, we use this structure to calculate the electron-phonon coupling coefficients and thermodynamic properties of $(MoS_2)_2Ca$ and $(WS_2)_2Ca$ in the superconducting state. At this point, we should mention that in the work of Somoano *et al.* [33], bulk Ca-intercalated molybdenum disulfide crystal was synthesized, characterized, and measured. As the authors found, Ca-intercalated MoS_2 crystallizes in an orthorhombic structure, which is in contrast to the hexagonal structure of pristine MoS_2 and alkali-metal-intercalated MoS_2 . The origin of this difference between bilayer and bulk structure is unknown; additional research is required.

Before calculating possible superconducting properties, we analyzed the electronic band structures of $(MoS_2)_2Ca$ and $(WS_2)_2Ca$. In Fig. 4, the band dispersion shows the metallic character of both systems. This means that after Ca-atoms intercalation of transition-metal dichalcogenides, we can observe the transition from semiconducting to the metallic phase [45].

To determine the thermodynamic properties of a conventional superconductor, the standard approach is to solve numerically the Eliashberg equations [46–49]:

$$\Delta_m Z_m = \pi k_B T \sum_n \frac{\lambda_{n,m} - \mu^* \theta (\omega_c - |\omega_n|)}{\sqrt{\omega_n^2 Z_n^2 + \varphi_n^2}} \varphi_n, \quad (1)$$

and

$$Z_m = 1 + \frac{\pi k_B T}{\omega_n} \sum_n \frac{\lambda_{n,m}}{\sqrt{\omega_n^2 Z_n^2 + \varphi_n^2}} \omega_n Z_n, \quad (2)$$

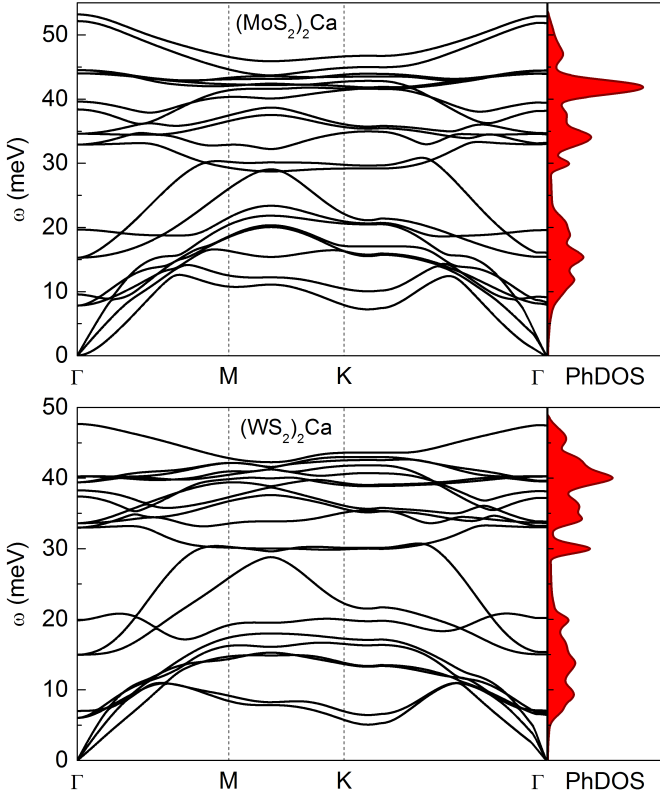


FIG. 3. Phonon dispersion and phonon density of states for Ca-intercalated bilayer MoS_2 and WS_2 .

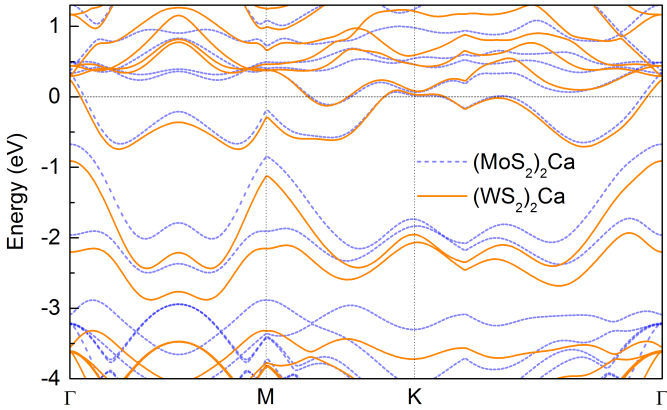


FIG. 4. Calculated electronic band structures of $(\text{MoS}_2)_2\text{Ca}$ (dashed blue lines) and $(\text{WS}_2)_2\text{Ca}$ (solid orange lines).

where the first equation is for the superconducting order parameter function and the second determines the electron effective mass. The pairing kernel for the electron-phonon interaction is given by:

$$\lambda_{n,m} = 2 \int_0^{\omega_D} d\omega \frac{\omega}{(\omega_n - \omega_m)^2 + \omega^2} \alpha^2 F(\omega). \quad (3)$$

k_B , μ^* , and θ denote the Boltzmann constant (0.0862 meV/K), the Coulomb pseudopotential (we use the com-

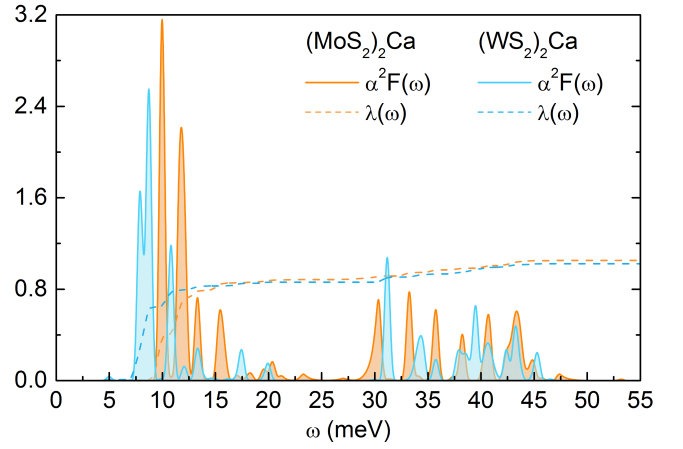


FIG. 5. Eliashberg spectral function $\alpha^2 F(\omega)$ and the cumulative electron-phonon coupling strength $\lambda(\omega)$ of Ca-intercalated bilayer MoS_2 and WS_2 .

monly accepted value of 0.1), and the Heaviside step function with cut-off frequency ω_c equal to three times the maximum phonon frequency ω_D . The Eliashberg spectral function $\alpha^2 F(\omega)$ is given by:

$$\alpha^2 F(\omega) = \frac{1}{2\pi N(\epsilon_F)} \sum_{\mathbf{q}v} \delta(\omega - \omega_{\mathbf{q}v}) \frac{\gamma_{\mathbf{q}v}}{\hbar\omega_{\mathbf{q}v}}, \quad (4)$$

where the line width of phonon mode v at the wave vector \mathbf{q} is defined as follows:

$$\gamma_{\mathbf{q}v} = 2\pi\omega_{\mathbf{q}v} \sum_{ij} \int \frac{d^3k}{\Omega_{BZ}} |g_{\mathbf{q}v}(\mathbf{k}, i, j)|^2 \delta(\epsilon_{\mathbf{q},i} - \epsilon_F) \times \delta(\epsilon_{\mathbf{k}+\mathbf{q},j} - \epsilon_F), \quad (5)$$

Symbol Ω_{BZ} refers to the value of the Brillouin zone, i and j are band indices, $\epsilon_{\mathbf{q},i}$ denotes the energy of the bare electronic Bloch state, and $g_{\mathbf{q}v}(\mathbf{k}, i, j)$ is the electron-phonon matrix element that can be determined in a self-consistent manner by the linear response theory. The shape of the Eliashberg function for Ca-intercalated bilayer molybdenum and tungsten disulfides are shown in Fig. 5. In addition, the frequency-dependent electron-phonon coupling, given by $\lambda(\omega) = 2 \int_0^{\omega_D} \omega^{-1} \alpha^2 F(\omega) d\omega$, is plotted using dashed lines. The obtained $\lambda(\omega_D) = 1.05$ for $(\text{MoS}_2)_2\text{Ca}$ and $\lambda(\omega_D) = 1.02$ for $(\text{WS}_2)_2\text{Ca}$ clearly indicates that we are dealing with strong-coupling superconductors.

The numerical solutions of 1 and 2 enable us to determine the condensation energy (E_{cond}) defined as a difference between the free energy of the normal state and that of the superconducting state in the absence of a magnetic field [47, 50]:

$$\frac{E_{\text{cond}}(T)}{N(\epsilon_F)} = -\pi T \sum_n \left(\sqrt{\omega_n^2 + \Delta_n^2} - |\omega_n| \right) \times \left(Z_n^N \frac{|\omega_n|}{\sqrt{\omega_n^2 + \Delta_n^2}} - Z_n^S \right), \quad (6)$$

where Z_n^N and Z_n^S denote the mass renormalization functions for the normal ($\Delta_m = 0$) and superconducting ($\Delta_m > 0$) states, respectively. In this study, the calculations of thermodynamics of phonon-mediated superconductors $(\text{MoS}_2)_2\text{Ca}$ and $(\text{WS}_2)_2\text{Ca}$ are based mostly on the results obtained for the condensation energy.

III. RESULTS AND DISCUSSION

From the physical point of view, the condensation energy denotes the energy that stabilizes the superconducting state. In Fig. 6(a), we plot the condensation energy as a function of temperature. We should note that at a temperature near zero, an excellent degree of accuracy is achieved with the following relationship $\Delta(0) = \sqrt{E_{\text{cond}}(0)}$, where $\Delta(0)$ is an energy gap at the Fermi level. The shapes of functions $\Delta^2(T)$ are plotted in Fig. 6(a) using a blue dashed line for $(\text{MoS}_2)_2\text{Ca}$ and red dashed line for $(\text{WS}_2)_2\text{Ca}$. As we can see, with an increase of temperature, the condensation energy decreases and vanishes like an energy gap function at critical temperatures equal to 13.3 K for $(\text{MoS}_2)_2\text{Ca}$ and 9.3 K for $(\text{WS}_2)_2\text{Ca}$. Here, we should mention that the recently studied Li-intercalated bilayer MoS_2 superconductor is characterized by a slightly lower critical temperature equal to 10.2 K [28]. In the case of tungsten disulfide, we expect that, even in the absence of experimental or other computational results used for comparison, the calcium is a good intercalant, and we hope that our results can be verified in the future.

Condensation energy is also related to the entropy difference (ΔS) as well as to the specific heat difference between the superconducting and normal states (ΔC). In particular, ΔS is determined by the first derivative of E_{cond} , and ΔC follows from the second derivative of E_{cond} :

$$\Delta S(T) = \frac{dE_{\text{cond}}}{dT} \quad \text{and} \quad \Delta C(T) = T \frac{d^2 E_{\text{cond}}}{dT^2}. \quad (7)$$

In Fig. 6(b), we can observe the behavior when an entropy difference appears between the superconducting and normal states. On this basis, we can conclude that the entropy of the superconducting state is lower than that of the normal state because of the ordering of electrons into pairs [51]. The plot of the specific heat difference between the superconducting and normal states on the temperature is presented in Fig. 6(c). The characteristic specific heat jump at the critical temperature is marked by the vertical line. In the next step, the thermodynamic critical field is calculated $H_C(T) = \sqrt{8\pi E_{\text{cond}}}$ and plotted in Fig. 7(a).

The estimated values of the energy gap at zero temperature, the specific heat jump at critical temperature, and the thermodynamic critical field at zero temperature allowed us to calculate three fundamental dimensionless ratios: $R_\Delta \equiv 2\Delta(0)/k_B T_C$, $R_C \equiv \Delta C(T_C)/C^N(T_C)$, and $R_H \equiv T_C C^N(T_C)/H_C^2(0)$, simultaneously. Here, the specific heat in the normal state is defined as $C^N = \gamma T$, where the Sommerfeld constant has the form: $\gamma \equiv (2/3)\pi^2 (1 + \lambda) k_B^2 N(\epsilon_F)$. Within the framework of the

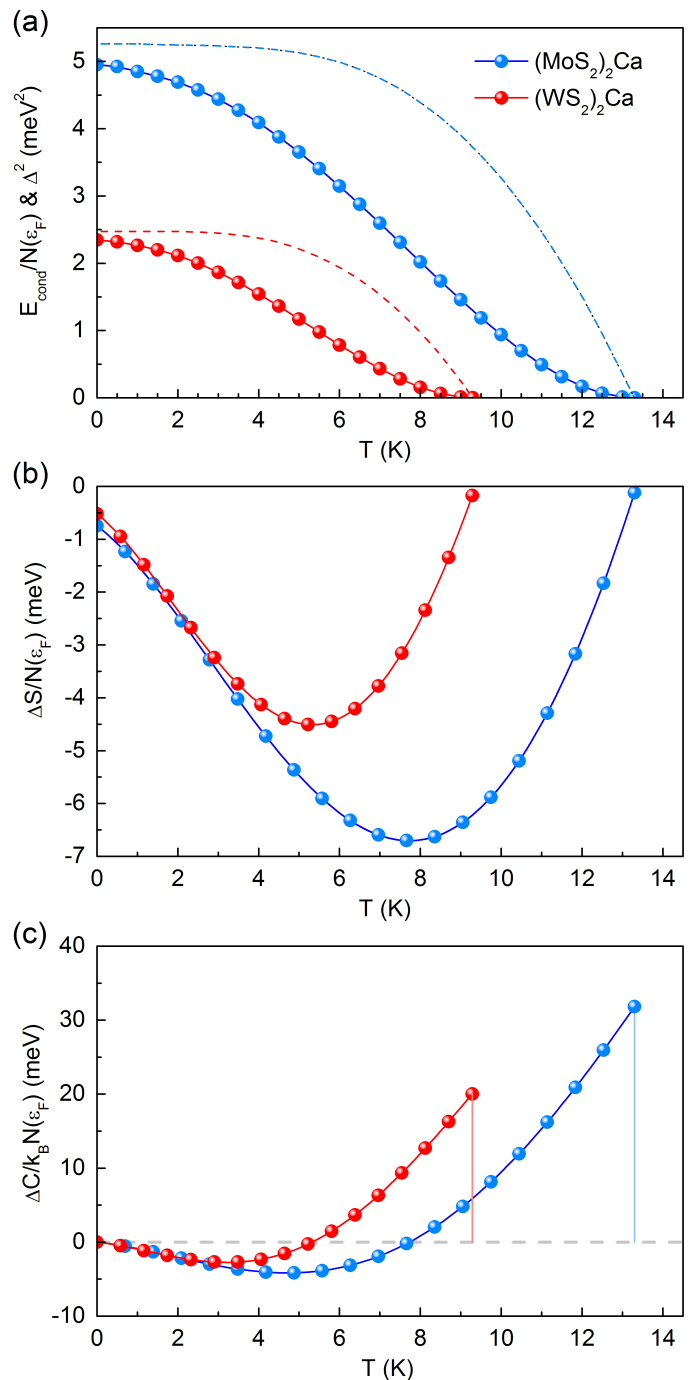


FIG. 6. a) Condensation energy (lines with symbols) combined with the energy gap function (dashed lines), b) entropy difference, and c) specific heat difference as a function of temperature.

BCS theory [52, 53], R_Δ , R_C , and R_H ratios adopt universal values equal to 3.53, 1.43, and 0.168, respectively [47]. The results obtained for the investigated superconductors are collected in Table I.

We can clearly see that the ratio of energy gap and specific heats as well as the ratio connected with the zero-temperature thermodynamic critical field exceed the pre-

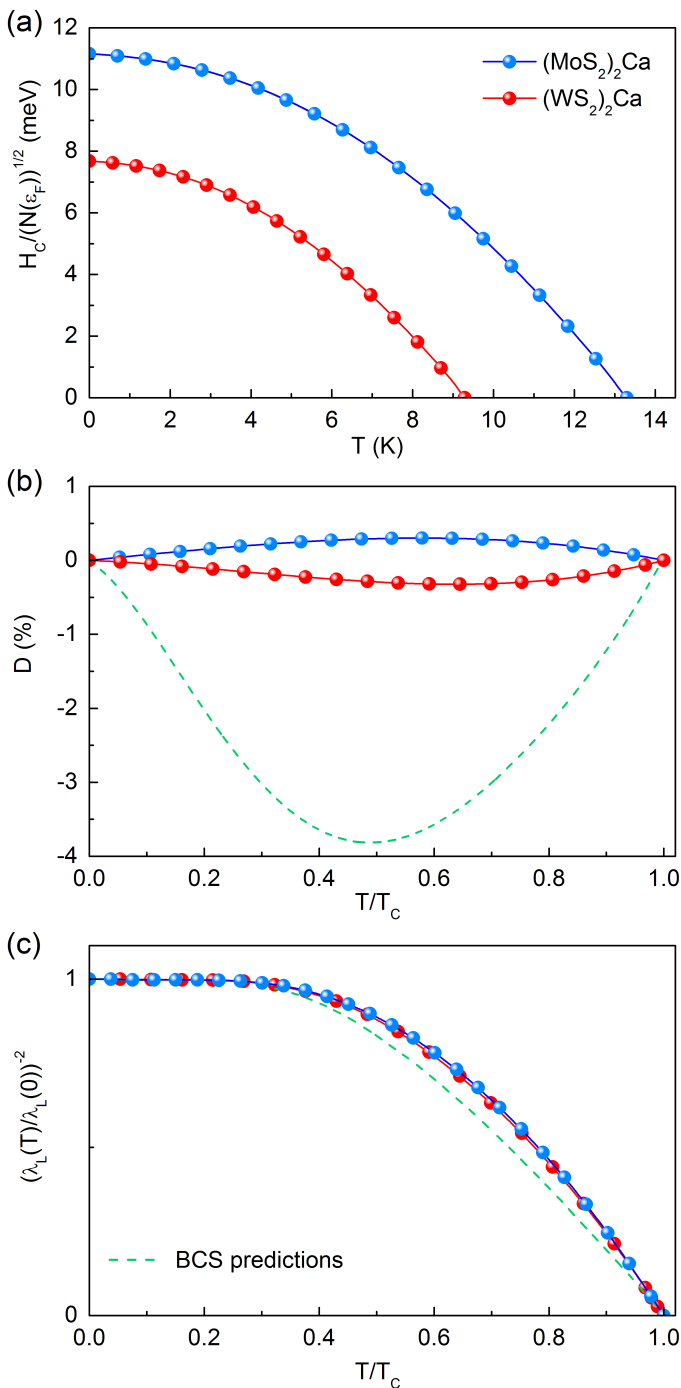


FIG. 7. a) Thermodynamic critical field, b) deviation of the thermodynamic critical field, and c) normalized London penetration depth as a function of temperature.

dictions of the BCS theory. The discrepancies between our results and the BCS estimates arise from the retardation and strong-coupling effects existing in the studied superconductors. We notice that these effects are well described within the framework of the Eliashberg formalism by the ratio $k_B T_C / \omega_{\text{ln}}$, where ω_{ln} is the logarithmic phonon frequency defined as: $\omega_{\text{ln}} \equiv \exp \left[\frac{2}{\lambda} \int_0^{+\infty} d\omega \frac{\alpha^2 F(\omega)}{\omega} \ln(\omega) \right]$.

TABLE I. Dimensionless ratios R_Δ , R_C , R_H , and $k_B T_C / \omega_{\text{ln}}$ of molybdenum and tungsten disulfide bilayers with Ca intercalation. The obtained results are compared with the respective BCS predictions.

	(MoS ₂) ₂ Ca	(WS ₂) ₂ Ca	BCS theory
R_Δ	4.00	3.94	3.53
R_C	2.04	1.89	1.43
R_H	0.145	0.147	0.168
$k_B T_C / \omega_{\text{ln}}$	0.083	0.070	0

The considered ratio equals 0.083 and 0.070 for molybdenum and tungsten disulfide bilayers with Ca intercalation, respectively, whereas the mean-field BCS theory is completely omitted (with the weak-coupling BCS limit, we have $k_B T_C / \omega_{\text{ln}} \rightarrow 0$).

Derogations from predictions of the BCS theory also can be observed in the shape of the thermodynamic critical field deviation function [47]:

$$D(T) = \frac{H_C(T)}{H_C(0)} - \left[1 - \left(\frac{T}{T_C} \right)^2 \right] \quad (8)$$

and London penetration depth (λ_L) [47]:

$$\frac{1}{e^2 v_F^2 \rho(0) \lambda_L^2(T)} = \frac{4\pi}{3\beta} \sum_{n=1}^M \frac{\Delta_n^2}{Z_n^S [\omega_n^2 + \Delta_n^2]^{3/2}}, \quad (9)$$

where e and v_F denote the electron charge and Fermi velocity, respectively. The obtained results compared with the BCS predictions are presented in Fig. 7(b) and Fig. 7(c).

IV. CONCLUSION

In this study, we performed comprehensive theoretical investigations on the possible existence of a superconducting state in molybdenum and tungsten disulfide bilayers with Ca intercalation. Combining density functional theory with the Migdal–Eliashberg formalism, we determined that Ca-intercalated bilayer MoS₂ and WS₂ exhibit a strong-coupling phonon-mediated superconductivity ($\lambda > 1$) with T_C of 13.3 and 9.3 K, respectively. In addition, we obtained direct evidence of non-BCS values of dimensionless ratios connected with thermodynamic functions. In particular, ratios of energy gap, specific heats, and that connected with the thermodynamic critical field significantly exceeded the values predicted by the conventional BCS theory. We identified these discrepancies when retardation and strong-coupling effects occurred in superconducting Ca-intercalated transition-metal dichalcogenide bilayers. We expect that (MoS₂)₂Ca and (WS₂)₂Ca can be successfully synthesized using chemical or physical methods and applied as nanoscale superconductors.

Acknowledgments

A.P. Durajski acknowledges the financial support under the scholarship START from the Foundation for Polish Science (FNP). All authors are grateful to the Czestochowa University of Technology—MSK CzestMAN for granting

access to the computing infrastructure built in the projects No. POIG.02.03.00-00-028/08 "PLATON - Science Services Platform" and No. POIG.02.03.00-00-110/13 "Deploying high-availability, critical services in Metropolitan Area Networks (MAN-HA)."

-
- [1] Yu Saito, Tsutomu Nojima, and Yoshihiro Iwasa, "Highly crystalline 2d superconductors," *Nat. Rev. Mater.* **2**, 16094 (2016).
- [2] Wonbong Choi, Nitin Choudhary, Gang Hee Han, Juhong Park, Deji Akinwande, and Young Hee Lee, "Recent development of two-dimensional transition metal dichalcogenides and their applications," *Mater. Today* **20**, 116 – 130 (2017).
- [3] Takashi Uchihashi, "Two-dimensional superconductors with atomic-scale thickness," *Supercond. Sci. Technol.* **30**, 013002 (2017).
- [4] Benjamin Sacepe, Thomas Dubouchet, Claude Chapelier, Marc Sanquer, Maoz Ovadia, Dan Shahar, Mikhail Feigelman, and Lev Ioffe, "Localization of preformed cooper pairs in disordered superconductors," *Nat. Phys.* **7**, 239244 (2011).
- [5] Yang Guo, Yan-Feng Zhang, Xin-Yu Bao, Tie-Zhu Han, Zhe Tang, Li-Xin Zhang, Wen-Guang Zhu, E. G. Wang, Qian Niu, Z. Q. Qiu, Jin-Feng Jia, Zhong-Xian Zhao, and Qi-Kun Xue, "Superconductivity modulated by quantum size effects," *Science* **306**, 1915–1917 (2004).
- [6] A P Durajski, "Effect of layer thickness on the superconducting properties in ultrathin pb films," *Supercond. Sci. Technol.* **28**, 095011 (2015).
- [7] E F Talantsev, W P Crump, J O Island, Ying Xing, Yi Sun, Jian Wang, and J L Tallon, "On the origin of critical temperature enhancement in atomically thin superconductors," *2D Mater.* **4**, 025072 (2017).
- [8] Allen M. Goldman and Nina Markovic, "Superconductor-insulator transitions in the two-dimensional limit," *Phys. Today* **51**, 39 (1998).
- [9] V.L. Berezinskii, "Destruction of long-range order in one-dimensional and two-dimensional systems having a continuous symmetry group. I. classical systems," *Sov. Phys. JETP* **32**, 493500 (1971).
- [10] V.L. Berezinskii, "Destruction of long-range order in one-dimensional and two-dimensional systems possessing a continuous symmetry group. II. quantum systems," *Sov. Phys. JETP* **34**, 610616 (1972).
- [11] J.M. Kosterlitz and D.J. Thouless, "Long range order and metastability in two dimensional solids and superfluids," *J.Phys. C Solid State Phys.* **5**, 124126 (1972).
- [12] Tingting Zhang, Shuang Wu, Rong Yang, and Guangyu Zhang, "Graphene: Nanostructure engineering and applications," *Front. Phys.* **12**, 127206 (2017).
- [13] Qing Hua Wang, Kourosch Kalantar-Zadeh, Andras Kis, Jonathan N. Coleman, and Michael S. Strano, "Electronics and optoelectronics of two-dimensional transition metal dichalcogenides," *Nat. Nanotechnol.* **7**, 699712 (2012).
- [14] Xidong Duan, Chen Wang, Anlian Pan, Ruqin Yu, and Xiangfeng Duan, "Two-dimensional transition metal dichalcogenides as atomically thin semiconductors: opportunities and challenges," *Chem. Soc. Rev.* **44**, 8859–8876 (2015).
- [15] Yuzheng Guo and John Robertson, "Band engineering in transition metal dichalcogenides: Stacked versus lateral heterostructures," *Appl. Phys. Lett.* **108**, 233104 (2016).
- [16] Dominik Szczęśniak, Ahmed Ennaoui, and Said Ahzi, "Complex band structures of transition metal dichalcogenide monolayers with spin-orbit coupling effects," *J. Phys.: Condens. Matter* **28**, 355301 (2016).
- [17] Ali Kandemir, Haluk Yapicioglu, Alper Kinaci, Tahir an, and Cem Sevik, "Thermal transport properties of MoS₂ and MoSe₂ monolayers," *Nanotechnology* **27**, 055703 (2016).
- [18] Pujun Zhao, Jiming Zheng, Ping Guo, Zhenyi Jiang, Like Cao, and Yun Wan, "Electronic and magnetic properties of re-doped single-layer MoS₂: A DFT study," *Comput. Mater. Sci.* **128**, 287 – 293 (2017).
- [19] K. K. Kam and B. A. Parkinson, "Detailed photocurrent spectroscopy of the semiconducting group vib transition metal dichalcogenides," *J. Phys. Chem.* **86**, 463–467 (1982).
- [20] Kin Fai Mak, Changgu Lee, James Hone, Jie Shan, and Tony F. Heinz, "Atomically thin MoS₂: A new direct-gap semiconductor," *Phys. Rev. Lett.* **105**, 136805 (2010).
- [21] Gang Luo, Zhuo-Zhi Zhang, Hai-Ou Li, Xiang-Xiang Song, Guang-Wei Deng, Gang Cao, Ming Xiao, and Guo-Ping Guo, "Quantum dot behavior in transition metal dichalcogenides nanostructures," *Front. Phys.* **12**, 128502 (2017).
- [22] K. S. Novoselov, A. K. Geim, S. V. Morozov, D. Jiang, Y. Zhang, S. V. Dubonos, I. V. Grigorieva, and A. A. Firsov, "Electric field effect in atomically thin carbon films," *Science* **306**, 666–669 (2004).
- [23] Jin-Wu Jiang, "Graphene versus MoS₂: A short review," *Front. Phys.* **10**, 287–302 (2015).
- [24] A P Durajski, "Influence of hole doping on the superconducting state in graphane," *Supercond. Sci. Technol.* **28**, 035002 (2015).
- [25] Xinyue Lin, Wentong Li, Yingying Dong, Chen Wang, Qi Chen, and Hui Zhang, "Two-dimensional metallic MoS₂: A dft study," *Comput. Mater. Sci.* **124**, 49 – 53 (2016).
- [26] Jelena Pesic, R Gajic, Kurt Hingerl, and Milivoj Belic, "Strain-enhanced superconductivity in Li-doped graphene," *Europhys. Lett.* **108**, 67005 (2014).
- [27] Jun-Jie Zhang, Bin Gao, and Shuai Dong, "Strain-enhanced superconductivity of MoX₂ (x = S or Se) bilayers with na intercalation," *Phys. Rev. B* **93**, 155430 (2016).
- [28] G. Q. Huang, Z. W. Xing, and D. Y. Xing, "Dynamical stability and superconductivity of Li-intercalated bilayer MoS₂: A first-principles prediction," *Phys. Rev. B* **93**, 104511 (2016).
- [29] Xin He, Hai Li, Zhiyong Zhu, Zhenyu Dai, Yang Yang, Peng Yang, Qiang Zhang, Peng Li, Udo Schwingenschlogl, and Xixiang Zhang, "Strain engineering in monolayer WS₂, MoS₂, and the WS₂/MoS₂ heterostructure," *Appl. Phys. Lett.* **109**, 173105 (2016).

- [30] J. T. Ye, Y. J. Zhang, R. Akashi, M. S. Bahramy, R. Arita, and Y. Iwasa, “Superconducting dome in a gate-tuned band insulator,” *Science* **338**, 1193–1196 (2012).
- [31] Avinash P. Nayak, Swastibrata Bhattacharyya, Jie Zhu, Jin Liu, Xiang Wu, Tribhuvan Pandey, Changqing Jin, Abhishek K. Singh, Deji Akinwande, and Jung-Fu Lin, “Pressure-induced semiconducting to metallic transition in multilayered molybdenum disulphide,” *Nature Commun.* **5**, 3731 (2014).
- [32] Zhenhua Chi, Feihsiang Yen, Feng Peng, Jinlong Zhu, Yijin Zhang, Xuliang Chen, Zhaorong Yang, Xiaodi Liu, Yanming Ma, Yusheng Zhao, Tomoko Kagayama, and Yoshihiro Iwasa, “Ultrahigh pressure superconductivity in molybdenum disulfide,” arXiv:1503.05331 (2015).
- [33] R. B. Somoano, V. Hadek, and A. Rembaum, “Alkali metal intercalates of molybdenum disulfide,” *J. Chem. Phys.* **58**, 697–701 (1973).
- [34] R. B. Somoano, V. Hadek, A. Rembaum, S. Samson, and J. A. Woollam, “The alkaline earth intercalates of molybdenum disulfide,” *J. Chem. Phys.* **62**, 1068–1073 (1975).
- [35] “Superconducting critical fields of alkali and alkaline-earth intercalates of MoS₂, author = Woollam, John A. and Somoano, Robert B., journal = Phys. Rev. B, volume = 13, pages = 3843–3853, year = 1976,” .
- [36] G. Q. Huang, Z. W. Xing, and D. Y. Xing, “Prediction of superconductivity in li-intercalated bilayer phosphorene,” *Appl. Phys. Lett.* **106**, 113107 (2015).
- [37] Yu Saito, Tsutomu Nojima, and Yoshihiro Iwasa, “Gate-induced superconductivity in two-dimensional atomic crystals,” *Supercond. Sci. Technol.* **29**, 093001 (2016).
- [38] D Szcześniak, A P Durajski, and R Szcześniak, “Influence of lithium doping on the thermodynamic properties of graphene based superconductors,” *J. Phys.: Condens. Matter* **26**, 255701 (2014).
- [39] Satoru Ichinokura, Katsuaki Sugawara, Akari Takayama, Takashi Takahashi, and Shuji Hasegawa, “Superconducting calcium-intercalated bilayer graphene,” *ACS Nano* **10**, 2761–2765 (2016).
- [40] J. Chapman, Y. Su, C. A. Howard, D. Kundys, A. N. Grigorenko, F. Guinea, A. K. Geim, I. V. Grigorieva, and R. R. Nair, “Superconductivity in Ca-doped graphene laminates,” *Sci. Rep.* **6**, 23254 (2016).
- [41] P. Giannozzi, S. Baroni, N. Bonini, M. Calandra, R. Car, C. Cavazzoni, D. Ceresoli, G. L. Chiarotti, M. Cococcioni, I. Dabo, A. D. Corso, S. de Gironcoli, S. Fabris, G. Fratesi, and R. Gebauer, “QUANTUM ESPRESSO: a modular and open-source software project for quantum simulations of materials,” *J. Phys. Condens. Matter* **21**, 395502 (2009).
- [42] Feliciano Giustino, “Electron-phonon interactions from first principles,” *Rev. Mod. Phys.* **89**, 015003 (2017).
- [43] Feliciano Giustino, *Materials modelling using density functional theory. Properties and predictions* (Oxford University Press, Oxford, 2014).
- [44] J. L. Verble and T. J. Wieting, “Lattice mode degeneracy in MoS₂ and other layer compounds,” *Phys. Rev. Lett.* **25**, 362–365 (1970).
- [45] R. Szcześniak, A.P. Durajski, and M.W. Jarosik, “Metallization and superconductivity in Ca-intercalated bilayer mos₂,” *J. Phys. Chem. Solids* **111**, 254 – 257 (2017).
- [46] G. M. Eliashberg, “Interactions between electrons and lattice vibrations in a superconductor,” *Soviet Physics JETP* **11**, 696 (1960).
- [47] J. P. Carbotte, “Properties of boson-exchange superconductors,” *Rev. Mod. Phys.* **62**, 1027 (1990).
- [48] R. Szcześniak, “The numerical solution of the imaginary-axis Eliashberg equations,” *Acta Phys. Pol. A* **109**, 179 (2006).
- [49] R. Szcześniak and A. P. Durajski, “Superconductivity well above room temperature in compressed MgH₆,” *Front. Phys.* **11**, 117406 (2016).
- [50] J.P. Carbotte and P. Vashishta, “Condensation energy of a superconductor,” *Phys. Lett. A* **33**, 227 – 228 (1970).
- [51] J. Sólyom, *Fundamentals of the Physics of Solids: Volume 3 - Normal, Broken-Symmetry, and Correlated Systems* (Springer, 2011).
- [52] J. Bardeen, L. N. Cooper, and J. R. Schrieffer, “Microscopic theory of superconductivity,” *Phys. Rev.* **106**, 162 (1957).
- [53] J. Bardeen, L. N. Cooper, and J. R. Schrieffer, “Theory of superconductivity,” *Phys. Rev.* **108**, 1175 (1957).